


Alpha-Taxilin: A Potential Diagnosis and Therapeutics Target in Rheumatoid Arthritis Which Interacts with Key Glycolytic Enzymes Associated with Metabolic Shifts in Fibroblast-Like Synoviocytes

Ashish Sarkar^{1,2}, Debolina Chakraborty^{1,2}, Swati Malik^{1,2}, Sonia Mann¹, Prachi Agnihotri^{1,2}, Monu Monu^{1,2}, Vijay Kumar³, Sagarika Biswas^{1,2} 

¹Council of Scientific & Industrial Research (CSIR), Institute of Genomics and Integrative Biology, Delhi University Campus, Delhi, 110007, India; ²Academy of Scientific and Innovative Research (AcSIR), Ghaziabad, Uttar Pradesh, 201002, India; ³All India Institute of Medical Sciences (AIIMS), New Delhi, 110029, India

Correspondence: Sagarika Biswas, Council of Scientific & Industrial Research (CSIR), Institute of Genomics and Integrative Biology, Delhi University Campus, Delhi, 110007, India, Tel +91-11-27662581, Email sagarika.biswas@igib.res.in

Background: Rheumatoid Arthritis (RA) is a chronic multifactorial inflammatory autoimmune disease of the synovial joint with unknown etiology. In our previous study, we identified Alpha-Taxilin (α -Taxilin) as one of the upregulated proteins in RA and validated it in different biological samples such as tissue, synovial fluid, and blood cells. Here we further investigated its mechanistic role in RA pathophysiology.

Methods: The α -Taxilin was validated in a larger cohort ($n = 106$) of RA plasma by Enzyme-linked Immunosorbent Assay (ELISA). Interacting proteins were identified by co-immunoprecipitation followed by mass spectrometry, and in silico analyses were done to identify protein-protein interactions and involved pathways. The in vitro knockdown studies were performed on SW982 cells and Rheumatoid Arthritis Fibroblast-like Synoviocyte (RAFLS) to investigate the molecular mechanism of α -Taxilin involved in RA via Western Blot, quantitative real-time polymerase chain reaction (qRT-PCR), and confocal microscopy, which was further validated by in vivo studies via collagen-induced arthritis (CIA) rat model.

Results: The plasma level of α -Taxilin was found to be significantly increased in plasma samples from patients with RA compared to osteoarthritis (OA), systemic lupus erythematosus (SLE), and healthy controls (HC). The α -Taxilin was found to be positively correlated with anti-citrullinated peptide antibody (ACPA) levels and DAS score in patients with RA. Seventeen interacting proteins were identified with α -Taxilin, and in silico study suggested that glycolysis and gluconeogenesis pathways are the most affected pathways regulated by α -Taxilin. The in vitro knockdown studies of α -Taxilin resulted in decreased levels of pro-inflammatory cytokines, p65, reactive oxygen species (ROS), and toll-like receptors (TLRs). It also improved macroscopic arthritic score, paw edema, and inflammation in CIA rats.

Conclusion: α -Taxilin has been found to be associated with glycolysis and gluconeogenesis. This may lead to a metabolic shift in synovial cells, ROS generation, and TLR activation. Therefore, α -Taxilin can be targeted for its diagnostic and therapeutic potential in RA along with other parameters.

Keywords: toll-like receptor, rheumatoid arthritis, inflammation, metabolic shift, glycolysis, pyruvate metabolism

Introduction

Rheumatoid arthritis (RA) is the most common chronic, systemic inflammatory autoimmune disease of joints, affecting around 1% of the population worldwide.¹ It stood at 42nd ranks among 291 contributors to the disability index and

contributed to modest global disability.² The risk factors affect the immune cells to produce self-antigens, which enables the production of autoantibodies and anti-citrullinated protein antibodies (ACPA), causing inflammation and joint destruction.¹

Despite many efforts, the etiology of RA is still not understood well.¹ Manifestation of RA is marked by inflammation of the synovial membrane and articular tissue caused by the participation of immune cells (T cells, B cells, dendritic cells, macrophages, neutrophils) and non-immune cells (fibroblasts and chondrocytes). Secretion of pro-inflammatory cytokines such as Interleukin-6 (IL-6), Tumor Necrosis Factor- α (TNF- α), and Interleukin-1 β (IL-1 β) by activation of signaling pathways³ majorly Nuclear Factor kappa B (NF- κ B) and a mitogen-activated protein kinase (MAPK)⁴ in the osteoclasts. Currently, anti-cyclic citrullinated peptide (anti-CCP), and rheumatoid factor (RF) are used to diagnose the disease. However lack of specificity makes the diagnosis critical, leading to irreversible joint damage.^{5,6} Symptomatic treatment mainly involves nonsteroidal anti-inflammatory agents (NSAIDs), disease-modifying anti-rheumatic drugs (DMARDs), and biologics in coalition with proper rest, exercise, and, in severe cases, surgery improves the lifestyle of patients.⁷ However, continuous consumption of these drugs over a long period of time causes side effects such as renal failure, liver toxicity, and cytopenia.⁸ Thus, novel and more precise diagnostic tools are essentially needed. Although tremendous effort has been made to identify a few marker proteins using biological samples such as plasma,⁹ synovial fluid (SF),¹⁰ and synovium,¹¹ clinical diagnosis of RA remains challenging due to the lack of specificity.

Synovitis is the main pathological feature of RA and fibroblast-like synoviocyte (FLS) is the most important component of the inflamed synovial membrane.¹² Recent evidence suggests that these FLS exhibit significant alteration in glucose, lipid, and amino acid metabolism before synovitis onset. It suggests that, activation of immune cells and cytokines promotes these FLS into metabolic abnormality and pro-inflammatory phenotype.¹³ The dysregulated blood vessels in inflamed synovium and increased demand for oxygen by infiltrating immune cells leads to the switching of FLS to a highly metabolically active state, which further exacerbates the inflammatory response.¹³ Further, metabolomics study shows that glucose metabolism and glycolytic intermediates are associated with a phenotypic change in FLS, as well as early-stage disease onset.¹⁴ Studies also show improvement by targeting metabolic shift not only in FLS aggressive phenotype, but also in bone and cartilage degradation in various animal models suggesting an important role of a metabolic shift in FLS in mediating inflammation in RA.¹⁴ Previous studies suggest that fibroblast present in SF closely resemble the pathological sub-lining layer of FLS subset in terms of surface protein expression, leukocyte cross-talk, and cytokine production in RA inflammation.¹⁵ In our previous study, we focused our investigation on synovial fluid cells and identified a novel potential disease-associated protein α -Taxilin, known as Interleukin-14- α (IL-14 α) or Taxilin- α having gene symbol “TXLNA”, significantly upregulated in RA using a proteomic approach.¹⁶ It has a long coiled-coil region in its C-terminal half and shares a homologous coiled-coil structure with β -Taxilin and γ -Taxilin.¹⁷

The α -Taxilin is linked to renal cell carcinoma, hepatitis B, autoimmunity, and intracellular vesicle trafficking.^{17,18} Interestingly, α -Taxilin also interacts with the syntaxin family such as Syntaxin-3 (STX3) and Syntaxin-4 (STX4),¹⁹ which are involved in pro-inflammatory cytokines through activation of Toll-like receptor-2 (TLR-2) and Toll-like receptor-4 (TLR-4) in immune cells.^{17,20} Reports showed that α -Taxilin, also known as a high molecular B cell growth factor, is secreted by activated T cells. The stimulation of α -Taxilin results in increased cyclic adenosine monophosphate (cAMP), which is well established as a potent regulator of innate and adaptive immune cell function.²¹ The study shows α -Taxilin also contributes to B cell memory in humans and extended B-cell populations in animals correlating with increased serum antibodies and susceptibility to autoimmune disease.²² However, there is a lack of clear understanding of its mechanistic involvement in inflammation and autoimmune disease. Strong expression of α -Taxilin was also detected in proliferating neuro-epithelial cells during embryonic development and found to be correlated with cell proliferation,²³ and RA is broadly diagnosed by proliferated synovial tissue, extending over the articular cartilage to the subchondral bone.²⁴ The inflammatory and immune responses to RA are also associated with extensive dramatic metabolic rewiring due to increased oxygen consumption, leading to the generation of reactive nitrogen and oxygen intermediates.²⁵ The above report thus led us to speculate that the upregulation of α -Taxilin in SF cells may have a potential diagnostic and therapeutic effect. Therefore, we investigated the molecular mechanism of α -Taxilin and its effects on pathways involved in mediating inflammation. We also investigated the possible utilization of α -Taxilin for diagnostic purposes and

validated its role via an in vitro study using rheumatoid arthritis fibroblast-like synoviocyte (RAFLS) cells and an in vivo study using a collagen-induced arthritis (CIA) rat model.

Methods

Sample Collection

All patients and healthy volunteers included in the study signed written consent before sample collection. A detailed demography has been provided in the supplementary data ([Supplementary Table ST1](#)). The study protocol complied with the Declaration of Helsinki and was approved by the Ethical Committee of the Council of Scientific & Industrial Research Institute of Genomics & Integrative Biology (CSIR-IGIB), New Delhi, India, and All India Institute of Medical Science (AIIMS), and New Delhi, India (CSIR-IGIB/IHEC/2017-18 Dt. 08.02.2018). Whole venous blood samples (\approx 4ml) from patients with RA (n = 106), Osteoarthritis (OA) (n = 96), systemic lupus erythematosus (SLE) (n = 8), and Healthy Control (HC) (n = 30) were collected in sterile ethylenediaminetetraacetic acid (EDTA)-coated vials (P-Tech, India). Biopsy synovium was collected from RA patients (n = 15) in Dulbecco's modified Eagle's medium (DMEM) (HiMedia, India) supplemented with 10% fetal bovine serum (FBS)(Gibco, USA) and 1% antibiotic solution (HiMedia, India). All patients included in the study fulfilled the American College of Rheumatology criteria for the diagnosis of RA. Patients with other comorbidities along with RA were excluded.

Enzyme-Linked Immunosorbent Assay

Plasma samples were separated by centrifuging blood samples at $1500\times g$ for 5 minutes (min) at 4 degree Celsius ($^{\circ}C$). The level of α -Taxilin was measured in RA (n = 106), OA (n = 96), HC (n = 30), and SLE (n = 8) patients using an enzyme-linked immunosorbent assay (ELISA) kit (Elabscience, USA), and the level of ACPA in plasma samples in patients with RA (n = 18) was measured using the ACPA ELISA kit (Fine test, USA). Plasma samples (8:2 dilution) were incubated for 3 hours (h), at $37^{\circ}C$, washed with wash buffer, incubated again (2h, $37^{\circ}C$) with 100 microliter (μ l) biotinylated α -Taxilin/anti-ACPA (1:100 dilution) primary antibody, washed again, and incubated (1h, $37^{\circ}C$) with 100 μ L (1:100 dilution) Horseradish Peroxidase (HRP)-conjugated secondary antibody. The substrate was then added and incubated (15min at $37^{\circ}C$), the reaction was stopped with stop solution, and absorbance was measured at 462 nanometer (nm) using a Spectra Max plus 384 (Molecular devices, USA).²⁶ The concentration of α -Taxilin was measured in RA, OA, HC, and SLE using the standard curve generated by pure α -Taxilin concentration with respect to optical density as per the protocol (Provided). The receiver operating characteristic (ROC) curve, area under curve (AUC), and coefficient of correlation (r) were generated using Prism software (GraphPad, USA).

SW982 Synovial Sarcoma Cell Culture Treatment and in vitro Knockdown of α -Taxilin

The synovial sarcoma cell line SW982 is a widely used synovial cell line used to mimic the RA-like inflammation in vitro, purchased from the American Type Culture Collection (ATCC), and maintained for five passages. Cells were cultured in six-well plates (Nunc, USA), incubated (5% CO_2 , $37^{\circ}C$), supplemented with 10% Fetal bovine serum (FBS) (Gibco, USA) and 1% antibiotic solution (HiMedia, India). Inflammation was induced with different doses of recombinant TNF- α (1, 5, 10, 20, and 40 nanogram (ng)/milliliter (ml) (Gibco, USA), and α -Taxilin expression levels were checked.^{27,28} The knockdown effect of α -Taxilin was further evaluated on inflammatory parameters after transfection with 25 nanomolar (nM) α -Taxilin siRNA (siTaxilin, Santa Cruz Biotechnology, USA) using lipofectamine RNAiMAX (Thermo Fisher, USA) to knockdown α -Taxilin.²¹ The α -Taxilin siRNA is a pool of 3 target-specific 19–25 nucleotide siRNAs, designed to knockdown α -Taxilin. After knockdown, the cells were induced with 20ng/ml TNF- α for 3h to mimic the RA-like in vitro conditions.²⁹ In this experiment, different combinations of treatment in SW982 were; VC: treatment with only transfection reagent; NS+TNF: 25nM non-targeted siRNA pool + recombinant TNF (20ng/ml); siTaxilin + TNF: 25nM siRNA (siTaxilin) + recombinant TNF (20ng/ml); VC+ TNF: treatment with only transfection reagent + recombinant TNF (20ng/ml).

Cell Proliferation Assay

To evaluate the cytotoxicity of recombinant TNF- α , and α -Taxilin, the 3-[4, 5-dimethylthiazol-2-yl]-2, 5 diphenyl tetrazolium bromide (MTT) (Roche, USA) assay was performed using RAFLS and SW982 cells. Both cell lines (RAFLS and SW982) were cultured in 96-well culture plates and treated with different doses of TNF- α (1, 5, 10, 20, and 40ng/ml)/ α -Taxilin (0, 6.25, 12.5, 25, 50, and 100ng/ml). The positive control group was incubated (3h) with 5% dimethyl sulfoxide (DMSO) (Sigma, USA), MTT 10 microliter (μ l) (2mg/ml solution) was then added to each well, incubated (2h), and the absorbance was measured at 570nm.³⁰

Isolation of RA Primary Cells from Biopsy Synovium and Treatment

The RA biopsy synovium (\approx 4–5 grams) was washed, finely chopped, treated with collagenase (0.5mg/g), and incubated for 12–18h in 30 ml complete media to obtain RAFLS. The undigested tissue was passed through a cell strainer having 100 micron (μ) pore size (BD Biosciences, USA), centrifuged at 500 \times g for 5min, and cultured in a T-75 tissue culture flask (Nunc, USA) in complete media. The cells were used in 3rd to 5th passages. The RAFLS cells were validated by morphological observation, vimentin expression, and p65 protein level ([Supplementary data Figure S1](#)). The cells were then treated with different doses (0, 6.25, 12.5, 25, 50, and 100ng/ml) of recombinant α -Taxilin (Aprent antigen, USA) to determine the effective dose of α -Taxilin on the NF- κ B p65 (Santa Cruz Biotechnology, USA) level. The different combinations of treatment in RAFLS were; UT: untreated cells; NS: 25nM non-targeted siRNA pool; siTaxilin: 25nM siRNA (siTaxilin); VC+ α -Taxilin: treatment with only transfection reagent + recombinant α -Taxilin protein; VC+ TNF: treatment with only transfection reagent + recombinant TNF (20ng/ml).

Western Blot

For Western-Blot (WB) cells (SW982 and RAFLS) were washed with phosphate buffer saline (PBS), and lysed with radioimmunoprecipitation assay (RIPA) (Thermo, USA) lysis buffer containing 1% (v/v) protease and phosphatase inhibitor cocktail (Gibco, USA), and incubated (1h at 4°C). The lysate was centrifuged (15,000 \times g, 4°C, 30 min), and protein 40 microgram (μ g) estimated by bicinchoninic acid assay (BCA) (G-biosciences, USA) was run on sodium dodecyl sulfate-polyacrylamide gel electrophoresis (SDS-PAGE) and transferred onto a nitrocellulose membrane (NC) (G-biosciences, USA) using a semi dry transfer unit (Bio-Rad, USA). The membranes were then incubated (4°C overnight) with 5% Bovine Serum Albumin (BSA), followed by washing and incubation (overnight at 4°C) separately with diluted (1:3000) primary antibodies; Anti-p-65 (Santa Cruz, USA), anti- α -Taxilin (Santa Cruz, USA), anti- glyceraldehyde-3-phosphate dehydrogenase (GAPDH) (Santa Cruz, USA), anti-STX-3 (Santa Cruz, USA), anti-STX-4 (Santa Cruz, USA), anti-TLR-4 (Cloud-Clone, USA), and anti-TLR-2 (Cloud-Clone, USA). Each NC membrane was then incubated for 3h at room temperature (RT) except for TLR-2 and TLR-4 antibodies, which were incubated overnight at 4°C as standardized.³¹ The membrane was washed and incubated (1h, RT) with HRP-conjugated anti-mouse secondary antibody (1:6000) (Jackson ImmunoResearch, USA), developed with an enhanced chemiluminescence reagent (Cyanogen, USA) obtained from Chemidoc MP (Bio-Rad, USA), and analyzed using Image Lab software (Bio-Rad, USA).¹⁶

Ribose Nucleic Acid Isolation and Quantitative Reverse Transcription Polymerase Chain Reaction

For quantitative reverse transcription polymerase chain reaction (qRT-PCR), the cells were lysed with 500 μ l TRIzol (G-bioscience, USA), incubated (5min, RT), added 200 μ l chloroform (MercUSA), and then centrifuged (15min, 11,000 \times g, 4°C). The top layer was aspirated, mixed with chilled isopropanol, and incubated on ice (10min), followed by centrifugation (15min at 11,000 \times g at 4°C). Ribose nucleic acid (RNA) pellets thus obtained were washed with 75% ethanol thrice, dissolved in nuclease-free water, and concentration was measured using a NanoDrop spectrophotometer (Thermo, USA). Complementary deoxyribose nucleic acid (cDNA) was then synthesized²² using kit (G Bioscience, USA), used for amplification of *TNF- α* , *IL-1 β* , *IL-6*, and *TXLNA* using the respective primers and EvaGreen master mix (G Bioscience, USA).^{32–34} Polymerase chain reaction (PCR) was run for 40 cycles using

a light cycler-480 system (Roche, USA) and analyzed by the Δct method. The primer sequences used were provided in tabular form (Table 1).

Co-Immunoprecipitation and Protein Identification by Liquid Chromatography-Tandem Mass Spectrometry

SW982 cells were grown in T-25 culture flasks (Thermo Fisher Scientific, USA) and treated with TNF- α (20ng, 3h). The α -Taxilin was co-immunoprecipitated by affinity chromatography with other interacting proteins using a Pierce Co-immunoprecipitation (Co-IP) Kit (Thermo Fisher Scientific, USA). The cells were lysed and centrifuged (30min, 11,000 \times g, 4°C), and the supernatant was allowed to pass through control agarose beads. The antibody (α -Taxilin) was immobilized (3h, RT) on agarose beads,²⁸ washed, and eluted in native elution buffer (provided). Proteins (10 μ g) were digested with trypsin (1 μ g trypsin/20 μ g protein) (Promega, USA) and subjected to Liquid chromatography-tandem mass spectrometry (LC-MS/MS),³⁵ acquired MS/MS scans in the mass range 100–1,500m/z. The filling time for the isolation window used for MS scans was 250 milliseconds, and for MS/MS, the time set was 100 ms.²⁶

Gene Ontology and Kyoto Encyclopedia of Genes and Genomes Enrichment Analysis of Screened α -Taxilin Interacted Proteins

The interacting protein of α -Taxilin were screened based on score and p-value and were then uploaded in STRING 12.0 software. The retrieved protein-protein interaction network was then exported to Cytoscape (version 3.8.1) for enrichment analysis.²⁶ Gene Ontology (GO) and Kyoto Encyclopedia of Genes and Genomes (KEGG) pathways of the interacting proteins were retrieved, by selecting “Retrieve functional enrichment” in Cytoscape 3.8.1 to elucidate the GO and KEGG signaling pathways associated with α -Taxilin and its interacting proteins. The GO and KEGG pathways were filtered on the basis of p-value (≤ 0.05) and number of genes, and the top 10 GO, and KEGG pathways were plotted by using Graph pad 8. Cytoscape is an open software for projecting the interaction of biomolecule networks with high-throughput expression data and is used to unify the conceptual framework of the involved biological pathways.³⁶ The pathways (GO, and KEGG) were sorted on the basis of the lowest p-values ($p \leq 0.05$) and the highest number of genes involved in each pathway.

Table 1 List of Primer Sequence and Their Gene Names

S No.	Gene Symbol	Primer Sequence
1	<i>IL-6</i>	5'-GGTACATCCTCGACGGCATCT-3' 5'-GTGCCTCTTTGCTGCTTTC AC-3'
2	<i>TNF-α</i>	5'-CCCCAGGGACCTCTCTAATC-3' 5'-GGTTTGCTACAACATGGG CTACA-3'
3	<i>IL-1β</i>	5'-GACCTCTGCCCTCTGGATG-3' 5'-AGGTGCTCAGGTCATTCTCC-3'
4	<i>GAPDH</i>	5'-GAAGGTGAAGGTCGGAGTC-3' 5'-GAAGATGGTGATGGGA TTTC-3'
5	<i>LDHA</i>	5'-ATCTTGACCTACGTGGCTTGA-3' 5'-CCATACAGGCACACTGGAATCTC-3'
6	<i>PKM</i>	5'-CGAGCCTCAAGTCACTCCAC-3' 5'-GTGAGCAGACCTGCCAGACT-3'
7	<i>ALDOA</i>	5'-GTTATCAAATCCAAGGCGGTGT-3' 5'-AGTCAGCTCCGTCCTTCTGTAC-3'
8	<i>TXLNA</i>	5'-GGTTTGGGAAGGAGATCACG-3' 5'-GGAGCTTCATCTGCTTCTGTG-3'

Immunofluorescence and Confocal Microscopy

The RAFLS cells were grown on coverslips (Thermo Fisher Scientific) in 6 well plates. Cells were treated as; NS – transfected with non-specific siRNA pool, siTaxilin – cells transfected with 25nM siTaxilin, α -Taxilin – cells treated with recombinant α -Taxilin pure protein. After treatment, coverslip was washed, fixed with 4% paraformaldehyde (PFA) (Merck, USA), added quenched buffer (1% glycine for 5min), permeabilized with 0.1% Triton-X (Sigma, USA), blocked with 3% Bovine serum albumin (BSA) (Sigma, USA), and incubated overnight (4°C). The coverslip was then washed and incubated (1.5h) with diluted (1:300) primary antibodies; anti-TLR-2 and anti-TLR-4 (Santa Cruz Biotechnology, USA). After incubation, the coverslip was washed and incubated with Alexa Fluor 546 secondary antibody (Thermo Fisher, USA) along with 4', 6-diamidino-2-phenylindole (DAPI). The coverslip was then washed, and mounted on a glass slide with mounting media (Life Technology, USA). Images were acquired at 100X magnification using a Leica SP8 microscope (Leica, Germany) with gated excitation/emission (DAPI: 359/461 nm, Alexa Fluor: 561/572nm) in scanning mode and exported using LAS-X software (Leica Germany version 3.7.4) after background subtraction. The average intensity was measured using Image J software after converting to an 8-bit image format, and the average intensity was used to generate the graph using GraphPad Prism software.³⁷

Dichlorodihydrofluorescein Diacetate Cellular Reactive Oxygen Species Measurement

RAFLS cells were grown and treated as mentioned above. Additionally one more group of RAFLS cells was treated with recombinant pure TNF- α (20ng/ml) for 3h. Cells (1×10^6) were then incubated (30 min) with 10 μ M Dichlorodihydrofluorescein diacetate (DCFDA) (Abcam, USA) solution, washed, and fluorescence images were obtained using a ZOE Fluorescent Cell Imager (Bio-Rad, USA), which corresponds to the cellular Reactive Oxygen Species (ROS) level. Fluorescence intensity was analyzed using ImageJ software and normalized to cell count.³⁸

Development of a Collagen-Induced Arthritis Model and Treatment

Female Wistar rats of 4–6 weeks (80 g) were obtained from the Indian Council of Medical Research (ICMR), National Institute of Nutrition (NIN), Hyderabad, India. The rats were acclimatized for 2 weeks and fed a standard rodent chow diet and water. The experimental design was approved by the Institutional Animal Ethics Committee (IGIB/IAEC/3/3/ Mar 2023). Four groups were created consisting of six rats per group: 1) untreated group/HC, 2) CIA, 3) treated with non-specific Si-RNA+ CIA (NS+CIA), and 4) treated with siTaxilin, siTaxilin+CIA (siTaxilin+CIA). To induce CIA, collagen (Type II, 2mg/ml) from chicken (Sigma, USA) was mixed (1:1) with complete adjuvant (Sigma, USA) and injected into the rats (1 μ g/g of the body weight) subcutaneously proximal to the base of the tail on 1st and 14th day. siRNA (100ng/g) was then injected intraperitoneal (IP) 2 days prior to the induction of CIA and thereafter every 7th day till the 24th day with the help of in vivo fectamine.^{39,40} Rats were euthanized on the 28th day using a Thiopentone and Xylazine (3:1) cocktail (Sigma, USA). Blood and synovial tissue samples were collected for further analysis.

Paw Volume Measurement and Macroscopic Arthritis Score Calculation

The hind paw volumes of rats were measured on 1st, 7th, 14th, 21st, and 28th day using a plethysmometer (Harvard Apparatus, USA). The arthritic score was calculated based on the macroscopic observations of swelling, edema, and redness in all four paws of each rat. The scores were given on a scale of 1–4: severity, 1: no visible edema, swelling, and redness; 2: moderately involved joints; 3: highly involved joints with edema, redness, and swelling; and 4: joints severely affected by edema, swelling, and redness.⁴¹

Pro-Inflammatory Cytokines Level Detection in Rat Plasma

ELISA was performed (ELK Biotechnology, China), and the levels of cytokines (IL-6, TNF- α , and IL-1 β) were measured in rat plasma. Briefly, 100 μ l of plasma sample was added to the pre-coated ELISA plate (provided) along with the standard and incubated for 120min at 37°C. The plate was then washed and incubated (90min at 37°C) with a biotinylated primary antibody (anti-IL-6, anti-TNF- α , and anti-IL-1 β), followed by incubation at 37°C (40min). HRP-

conjugated secondary antibody was added to wells, incubated for 30min, washed after incubation and cytokine detection was performed using a chromophore substrate solution (provided). Absorbance was measured at 462 nm using a spectrometer (Molecular Devices).

Hematoxylin and Eosin Staining and Image Processing

Rat synovium was fixed in 10% formalin, dehydrated, and embedded in paraffin blocks. The blocks were cut into 5 μ thicknesses using a microtome, mounted on slides, deparaffinized, and stained with hematoxylin (1min). Slides were then decolorized, counter-stained with alcoholic eosin for 30 seconds (s), mounted with xylene on the slide, covered with a coverslip, and viewed using a Nikon ECLIPSE 90i microscope (Nikon, Japan).⁴² The Hematoxylin and Eosin (H&E) stained slide images were analyzed by Image-J (version 1.53t) software.

Statistical Analysis

All statistical analyses were performed using GraphPad Prism software (version 8.4.3). Student's t-tests were used to compare variables between two groups, and one-way Analysis of Variance (ANOVA) was used to compare variables among multiple groups. All bar graphs represent mean \pm standard deviation (SD), and data were obtained from at least three independent experiments.⁴³ The methods applied in the study have been summarized in a flow chart given in the supplementary data ([Supplementary data Figure S2](#)).

Results

Correlation of α -Taxilin with ACPA, and DAS Score in RA

The ELISA results revealed significantly upregulated (\approx 200pg/ml) concentrations of α -Taxilin in the RA (n = 106), compared to OA (100pg/ml), HC (\approx 100pg/ml), and SLE (\approx 80pg/ml) patient plasma samples ([Figure 1A](#)). The ROC curve of the ELISA indicates 90.63 specificity at 91.67 sensitivity with an AUC value of 0.97 for the ROC curve, which confirms that α -Taxilin level could be a potential diagnostic target ([Figure 1B](#)). Similar results were obtained using indirect ELISA ([Supplementary Figure S3](#)). The 2-fold increased concentration of α -Taxilin in RA patients compared to OA and SLE patients revealed that α -Taxilin is specifically upregulated by 2.22-fold, 3.566-fold, and 2.36-fold in RA compared to other inflammatory diseases such as OA, SLE, and HC, respectively. The results were further strengthened by conducting the correlation analysis of ACPA concentration in RA patients' plasma samples (n = 18), and Disease Activity Score (DAS) with the concentration of α -Taxilin, revealed a positive correlation for ACPA (coefficient of correlation, r = 0.63), and DAS (coefficient of correlation, r = 0.66) respectively in RA patients ([Figure 1C and D](#)).

TNF- α Induction Leads to Upregulation of α -Taxilin

Recombinant TNF- α was used to mimic RA-like conditions using the SW982 cell line. The WB results showed that α -Taxilin expression was increased with the increase in TNF- α doses (1–40ng/ml). At 20ng/ml of TNF- α , the maximum level of α -Taxilin expression was observed ([Figure 2A](#)), represented by densitometric analysis ([Figure 2B](#)). Furthermore, the effective time (3h) of TNF- α induction was selected based on the effective upregulation of mRNA level of α -Taxilin ([Supplementary Figure S4A](#)), pro-inflammatory cytokines *IL-1 β* , *TNF- α* , *IL-6* ([Supplementary Figure S4B–D](#) respectively), and NF-kB p65 protein expression ([Supplementary Figure S4E and F](#)). We then measured the cytotoxicity level based on the cell proliferation assay using MTT for different doses of TNF- α (1, 5, 10, 20, and 40ng/ml) and α -Taxilin (0, 6.25, 12.5, 25, 50, and 100ng/ml) in RAFLS, which revealed no significant cell death at any given dose ([Supplementary Figure S5A and B](#)). Hence the 20ng/ml dose of TNF- α for 3h was selected for further study.

Knockdown of α -Taxilin Ameliorates Pro-Inflammatory Cytokines

To determine the involvement of α -Taxilin in the inflammatory response, α -Taxilin was knocked down using 25nM siTaxilin (Santa Cruz, USA) in SW982 cells, and 62% inhibition was achieved ([Figure 2C](#)), based on densitometric analysis of WB ([Figure 2D](#)). The results showed that TNF- α induction led to an increase in the level of α -Taxilin; however, after α -Taxilin knockdown, TNF- α induction failed to reverse the level of α -Taxilin, suggesting that α -Taxilin

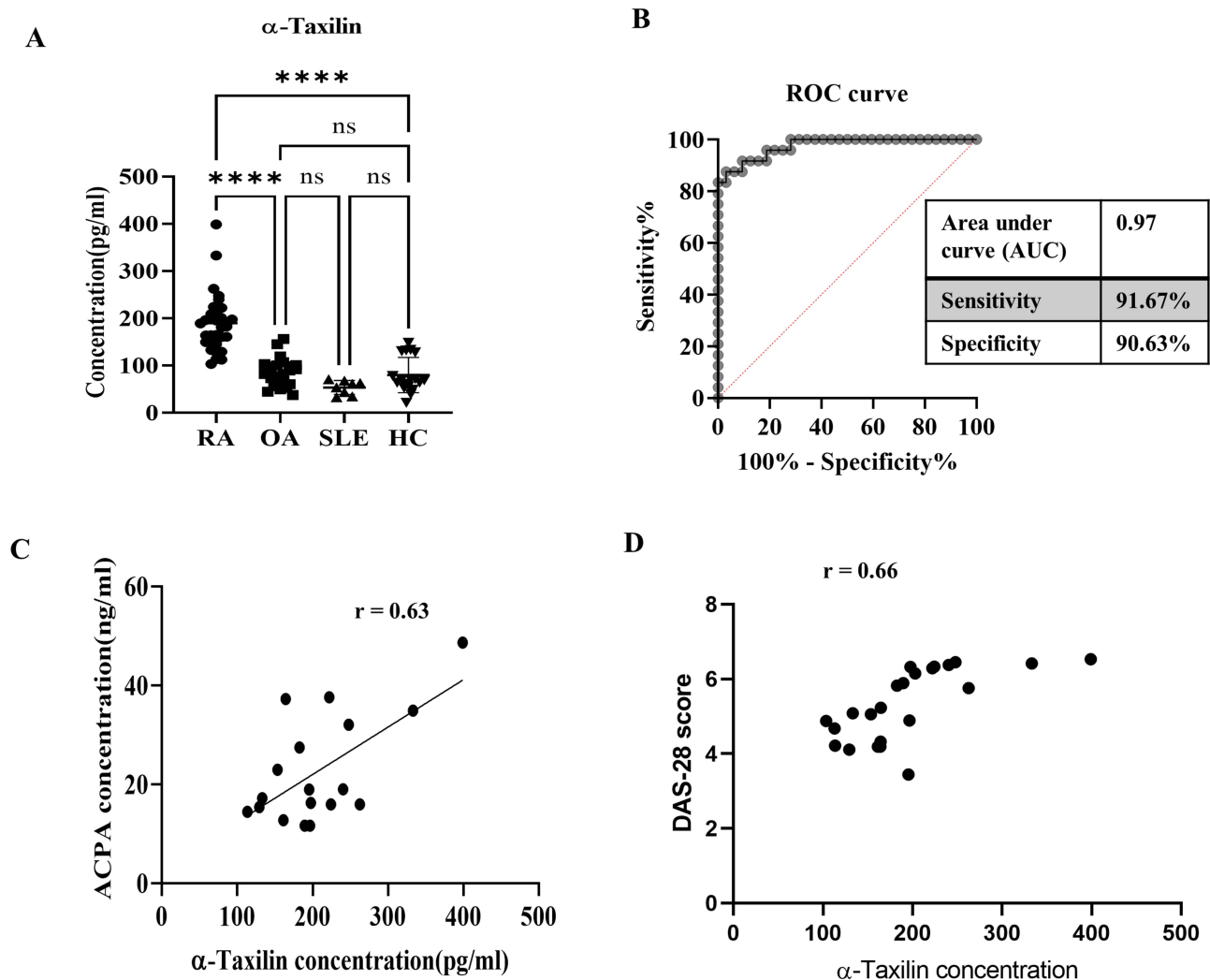


Figure 1 Concentration of α -Taxilin in RA compared to OA, SLE, and HC. **(A)** Graph showing the concentration of α -Taxilin in RA (n=106) compared to OA (n= 96), SLE (n=8), and HC (n=30) patients plasma samples. **(B)** The ROC curve shows the sensitivity and specificity of ELISA of α -Taxilin to distinguish RA from OA, SLE, and HC patients. **(C)** The graph represents the correlation of α -Taxilin concentration with ACPA level which shows a 0.63 Pearson coefficient indicating a positive correlation between ACPA and α -Taxilin in the RA (n=18) patient's plasma sample. **(D)** The graph represents the correlation of α -Taxilin concentration with DAS score in RA (n=18) which shows a 0.66 Pearson coefficient indicating a positive correlation between DAS and α -Taxilin. (**** $P \leq 0.0001$).

Abbreviations: RA, rheumatoid arthritis; OA, osteoarthritis; HC, healthy control; SLE, systemic lupus erythematosus; ROC, Receiver Operating Characteristic; r, correlation coefficient; ns, Non-significant; DAS, Disease Activity Score; ACPA, anti-citrullinated peptide antibody.

knockdown inhibits the effect of $TNF-\alpha$ (Figure 2E). Furthermore, mRNA levels of pro-inflammatory cytokines ($TNF-\alpha$, $IL-6$, and $IL-1\beta$) were significantly decreased by 0.42-fold, 0.85-fold, and 0.70-fold, respectively, in the knockdown group compared to those in the $TNF-\alpha$ -treated group (Figure 2F–H).

To validate the role of α -Taxilin, primary cells (RAFLS) were treated with different doses of recombinant α -Taxilin, and NF- κ B p65 levels were assessed using WB. The expression level of p65 was found to be increased with increasing doses of α -Taxilin, and the maximum expression was found at 50ng/ml (Figure 3A, upper panel), represented by densitometric analysis (Figure 3B), indicating that α -Taxilin induction leads to the activation of the inflammatory response, as p65 is the major downstream marker for NF- κ B activation. WB showed that the p65 level was significantly decreased in the siTaxilin-treated group compared to that of NS (Figure 3A, lower panel, and 3C), and increased significantly when cells were treated with $TNF-\alpha$ or α -Taxilin recombinant proteins (Figure 3A, lower panel, and 3C).

Our findings were further revealed that the knockdown of α -Taxilin in RAFLS reduced the mRNA levels of pro-inflammatory cytokines ($IL-6$, $TNF-\alpha$, and $IL-1\beta$) (Figure 3D–F), whereas the induction of recombinant α -Taxilin (50ng/

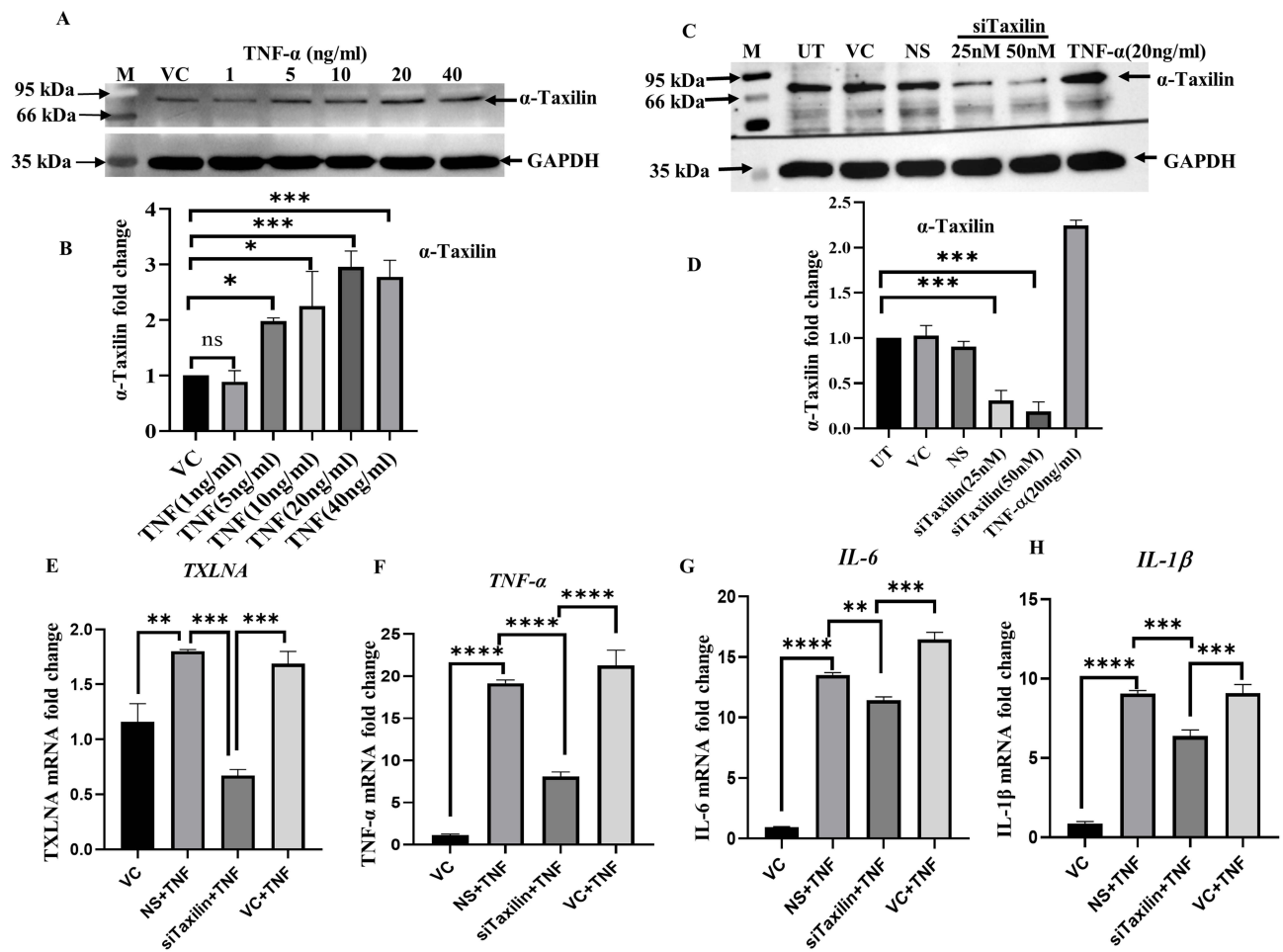


Figure 2 TNF- α induction upregulates α -Taxilin and inflammation in SW982 synovial cells. (A) The upper panel showing WB images of α -Taxilin after cells were treated with different doses (1, 5, 10, 20, and 40ng/ml) of TNF- α along with its respective GAPDH loading control (lower panel). (B) The graph represents the fold change of α -Taxilin based on the normalized densitometric value of WB upon different doses of TNF- α . (C) The panel showing WB images of α -Taxilin after transfection with different doses (25nM and 50nM) of Si-RNA along with GAPDH loading control (lower panel). (D) The bar graph represents the fold change of α -Taxilin expression based on densitometric values of WB after knockdown using 25nM and 50nM Si-RNA induction and 20ng/ml TNF- α induction along with non-specific Si-RNA control. (E) The α -Taxilin mRNA levels were calculated based on qRT-PCR and represented as a bar graph, α -Taxilin was found to be significantly downregulated when transfected with 25nM/ml siTaxilin. (F) The graph showing the fold change of TNF- α mRNA expression in different treated groups. (G) The graph showing fold change of IL-6 mRNA expression in different treated groups. (H) The graph showing fold change of IL-1 β mRNA expression in different treated groups. (* $P \leq 0.05$, ** $P \leq 0.01$, *** $P \leq 0.001$, **** $P \leq 0.0001$).

Abbreviations: WB, Western-blot; ns, Non-significant; NS, non-specific siRNA; TNF- α , Tumor necrosis factor- α ; IL-6, Interleukin-6; IL1 β , Interleukin-1- β ; VC, Vehicle Control; UT, Untreated; kDa, kilo Dalton; GAPDH, Glyceraldehyde 3-phosphate dehydrogenase; nM, Nano molar; ng, Nano gram; mL, milliliter.

ml) and TNF- α (20ng/ml) for 3 hours increases the expression levels of pro-inflammatory cytokines (IL-6, TNF- α , and IL-1 β) in primary RAFLS (Figure 3D–F).

Identification of α -Taxilin Interacting Proteins by Co-Immunoprecipitation

To identify the interacted protein associated with α -Taxilin in inflammatory conditions, various proteins co-immunoprecipitated with α -Taxilin were identified using the Co-IP technique followed by mass spectrometry analysis after cells were treated with TNF- α . The workflow is shown in a diagram along with a WB image showing the expression level of α -Taxilin in Elute, Wash, IgG control, and flow-through in Co-IP samples (Figure 4A). Seventeen unique proteins were identified in the TNF- α -induced group using LC-MS/MS after comparing the identified proteins with those in the untreated (UT) group (Table 2). The majority of the proteins identified in the Co-IP technique were associated with glycolysis pathways along with key enzyme presence such as Fructose-bisphosphate aldolase A, ATP synthase subunit beta, L-lactate dehydrogenase A, L-lactate dehydrogenase, and Pyruvate kinase among the identified proteins. Other proteins identified were Alpha-actinin-4, Myosin-9, Tubulin beta chain, and Tropomyosin alpha-1 chain, and Myosin regulatory light polypeptide 9 associated with the regulation of actin cytoskeleton.

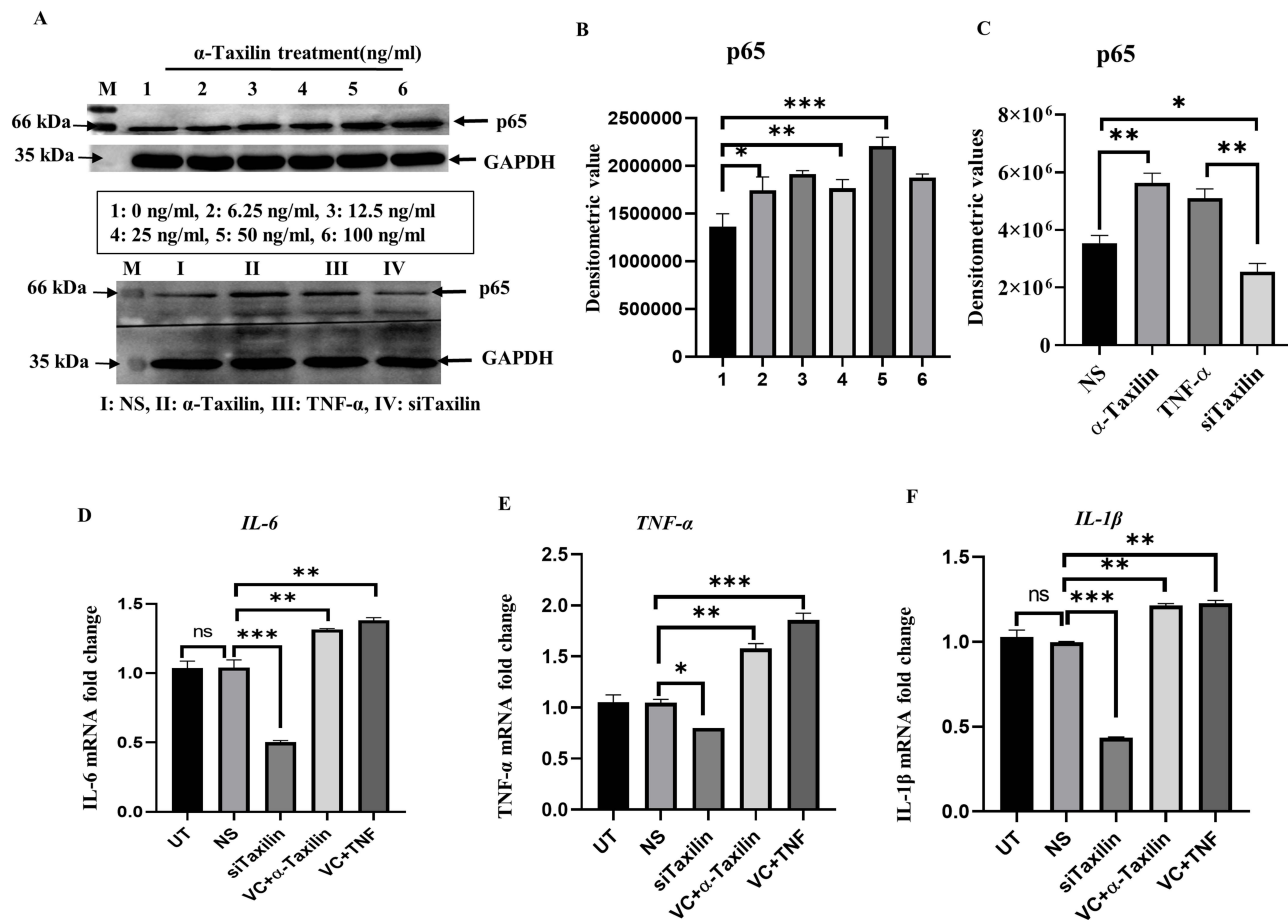


Figure 3 α -Taxilin ameliorated inflammation in primary RAFLS. (A) Upper panel showing WB image of NF- κ B p65 band along with GAPDH in different doses of α -Taxilin (1: 0ng/ml, 2: 6.25ng/ml, 3: 12.5ng/ml, 4: 25ng/ml, 5: 50 ng/ml, 6: 100ng/ml) induction, and the lower panel shows p-65 level along with GAPDH after knockdown of α -Taxilin (25nM) and induction of pure protein of α -Taxilin (50ng/ml) and TNF- α (20ng/ml). (B) Bar graph represents the densitometric values of p-65 level after different doses (1: 0ng/ml, 2: 6.25ng/ml, 3: 12.5ng/ml, 4: 25ng/ml, 5: 50ng/ml, 6: 100ng/ml) of α -Taxilin. (C) The bar graph represents p-65 level after knockdown of α -Taxilin and pure protein induction of TNF- α and α -Taxilin. (D) The bar graph represents IL-6 mRNA level after knockdown of α -Taxilin and pure protein induction of TNF- α and α -Taxilin along with control groups. (E) The bar graph represents TNF- α mRNA level after knockdown of α -Taxilin and pure protein induction of TNF- α and α -Taxilin along with control groups. (F) The bar graph represents IL-1 β mRNA level after knockdown of α -Taxilin and pure protein induction of TNF- α and α -Taxilin along with control groups. (* $P \leq 0.05$, ** $P \leq 0.01$, *** $P \leq 0.001$).

Abbreviations: WB, Western blot; ns, non-significant; NS, non-specific Si-RNA; TNF- α , tumor necrosis factor- α ; VC, vehicle control; UT, untreated; kDa, kilo Dalton; GAPDH, glyceraldehyde 3-phosphate dehydrogenase; IL-6, Interleukin-6; IL1 β , Interleukin-1- β ; nM, Nano molar; ng, Nano gram; mL, milliliter.

In silico Analysis Predict Glycolysis and Gluconeogenesis Pathway Involved in RA Like Inflammation

Advanced computer-based analytic tools have led in silico methods for evaluating and predicting pathways based on available databases.⁴⁴ The list of proteins (Table 2) was subjected to GO and KEGG pathway enrichment analysis, and a list of associated pathways was retrieved (Figure 4B). The top ten signaling pathways are shown in the graph, among which the glycolysis/gluconeogenesis and pyruvate metabolism pathways have the highest number of genes (Figure 4C). The genes involved were pyruvate kinase (PKM), fructose-bisphosphate aldolase A (ALDOA), and L-lactate dehydrogenase-A chain (LDHA) (Table 2), indicating that α -Taxilin might play a major role in regulating glycolytic metabolism during RA via these interacting proteins, which may lead to a metabolic shift.

Alpha-Taxilin Knockdown Leads to Decreased Levels of LDHA and PKM

The results of Co-IP, followed by protein identification by LC-MS/MS, revealed the upregulation of three major glycolytic enzymes, namely LDHA, PKM, and ALDOA. Knockdown of α -Taxilin revealed a significant reduction in the mRNA expression of LDHA and PKM in the siTaxilin-treated group compared to that in the NS group and an increase

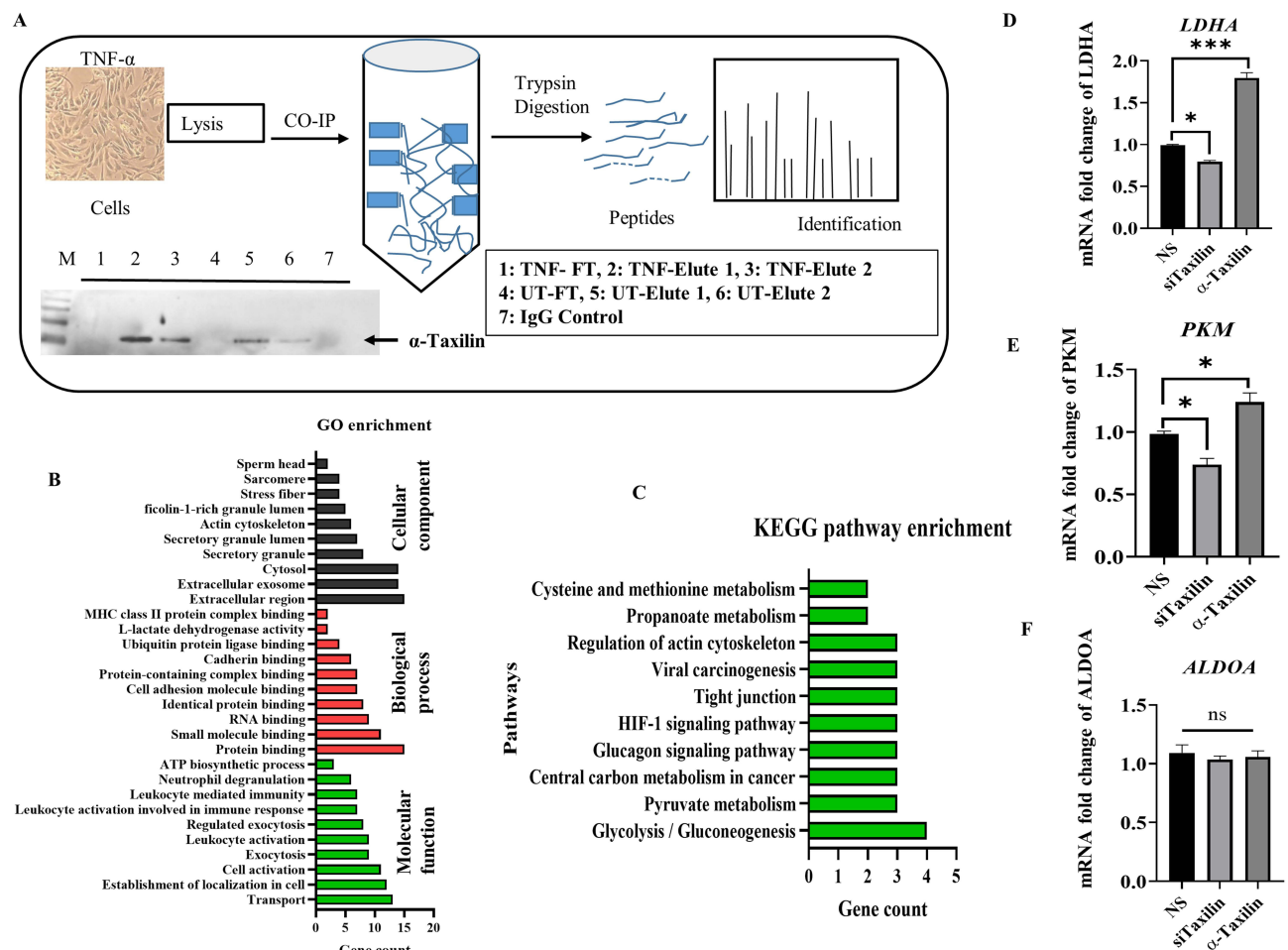


Figure 4 Involvement of α -Taxilin interacting proteins in glycolysis. **(A)** Image depicting a flow chart for protein identification using Co-IP technique where the WB image depicts α -Taxilin expression in flow-through and elution of Co-IP samples in UT and TNF- α treated cell lysate. **(B)** Graph showing the Gene-Ontology enrichment process, function, and pathway based on the identified proteins. **(C)** Graph showing KEGG pathway enrichment based on the identified protein where glycolysis/gluconeogenesis and pyruvate metabolism are the most affected pathways. **(D)** Expression of *LDHA* mRNA level in the siTaxilin treated group compared to NS and recombinant pure α -Taxilin group. **(E)** Expression of *PKM* mRNA level in the siTaxilin treated group compared to NS and recombinant pure α -Taxilin group. **(F)** Expression of *ALDOA* mRNA level in the siTaxilin treated group compared to NS and the recombinant pure α -Taxilin group. (* $P \leq 0.05$, *** $P \leq 0.001$).

Abbreviations: WB, Western blot; ns, non-significant; NS, non-specific siRNA; UT, untreated; Co-IP, co-immunoprecipitation; TNF, Tumor Necrosis Factor; IgG, Immunoglobulin; GO, Gene Ontology; KEGG, Kyoto Encyclopedia of Genes and Genomes.

in the mRNA expression of *LDHA* and *PKM* by 2-fold and 1.3-fold respectively in pure recombinant α -Taxilin treated group in RAFLS (Figure 4D and E). However, we did not observe any changes in *ALDOA* mRNA levels (Figure 4F).

Alpha-Taxilin Induces STX3, STX4, TLR-2, and TLR-4 Expression

The α -Taxilin, also known as a syntaxin-binding protein, binds *STX3* and *STX4* and activates toll-like receptors (*TLR-2* and *TLR-4*). To determine the pathway involved, the expression of *STX3*, *STX4*, *TLR-4*, and *TLR-2* was evaluated after the induction of RAFLS with α -Taxilin recombinant pure protein. Increased expression of *STX3*, *STX4*, *TLR-4*, and *TLR-2* with increasing doses of α -Taxilin was revealed by WB analysis (Figure 5A). Densitometric analysis of WB after normalization to GAPDH showed increased levels of *STX3* (Figure 5B), *STX4* (Figure 5C), *TLR-4* (Figure 5D), and *TLR-2* (Figure 5E). However, the fold change expression level (2.1-fold) of *TLR-2* was observed to be highest at lower doses (6.25ng/ml) and decreased the expression (0.62-fold) as the dose of α -Taxilin increased to 100ng compared to 6.25ng, and it remained significantly upregulated through all the doses compared to the untreated group (0ng/ml) (Figure 5E).

Table 2 List of Identified Unique Protein Co-Immunoprecipitated (Co-IP) with α -Taxilin Upon Given TNF- α Induction

S No	Protein Name	Accession	%COV	Peptides
1	Myosin-9	sp P35579 MYH9_HUMAN	39.8	50
2	Pyruvate kinase PKM	sp P14618 KPYM_HUMAN	51.04	17
3	Alpha-actinin-4	tr H7C144 H7C144_HUMAN	18.65	10
4	Putative elongation factor I-alpha	sp Q5VTE0 EF1A3_HUMAN	34.42	10
5	Elongation factor I-alpha I	tr A0A7I2V659 A0A7I2V659_HUMAN	34.64	10
6	Tubulin beta chain	sp P07437 TBB5_HUMAN	32.66	10
7	60 kDa heat shock protein, mitochondrial	sp P10809 CH60_HUMAN	15.01	6
8	I4-3-3 protein zeta/delta	sp P63104 I433Z_HUMAN	30.2	6
9	Fructose-bisphosphate aldolase A	sp P04075 ALDOA_HUMAN	28.57	6
10	ATP synthase subunit beta, mitochondrial	sp P06576 ATPB_HUMAN	21.55	5
11	Tropomyosin alpha-I chain (Fragment)	tr H0YKX5 H0YKX5_HUMAN	38.03	5
12	Glutathione S-transferase P	sp P09211 GSTP1_HUMAN	36.67	5
13	Heat shock protein HSP 90-beta	sp P08238 HS90B_HUMAN	14.36	4
14	L-lactate dehydrogenase A chain	sp P00338 LDHA_HUMAN	18.07	4
15	L-lactate dehydrogenase	tr A0A5F9ZHM4 A0A5F9ZHM4_HUMAN	14.96	3
16	40S ribosomal protein S18	tr Q5GGW2 Q5GGW2_HUMAN	44.12	2
17	Myosin regulatory light polypeptide 9	sp P24844 MYL9_HUMAN	55.81	6

To further validate our results, activation of TLRs (TLR-2 and TLR-4) was observed by confocal microscopy, and their localization in RAFLS was confirmed. The confocal image indicated that the expression of TLR-2 (Figure 6A) and TLR-4 (Figure 6B) both decreased significantly in the siTaxilin group (indicated in yellow) and both (TLR-2, and TLR-4) increased significantly (1.4-fold) when the RAFLS were treated with α -Taxilin as demonstrated by the densitometric graph using image analysis based on fluorescence intensity (Figure 6C and D).

Knockdown of α -Taxilin Reduces Dichlorodihydrofluorescein Diacetate Cellular, Reactive Oxygen Species in RAFLS

ROS production is one of the hallmarks of RA synovial inflammation, which leads to physiological and metabolic changes in cells. Since the activation of TLRs leads to inflammation and results in the generation of cellular ROS due to the metabolic shift of inflamed cells during disease conditions, DCFDA and cellular ROS generation was estimated.⁴⁵ The ROS production leading to increased oxidative stress is represented by the green color in the cells (Figure 6E). The level of fluorescence signal was analyzed by densitometric analysis (Figure 6F) and increased intracellular ROS production in TNF- α - and α -Taxilin-induced cells compared to that in NS control cells (2.1- and 1.96-fold, respectively) was observed. The siTaxilin-treated group showed significantly reduced (3.8-fold) ROS levels compared to the NS group (Figure 6F), indicating the role of α -Taxilin in intracellular ROS production.

Knockdown of α -Taxilin Results in Improved RA-Like Symptoms in CIA Rats

To mimic RA-like conditions, a widely used in vivo model of RA (CIA rat model) was generated. The hind paw volume was measured weekly from days 1 to 28, and a representative image taken on day 28 is shown in figure (Figure 7A, upper

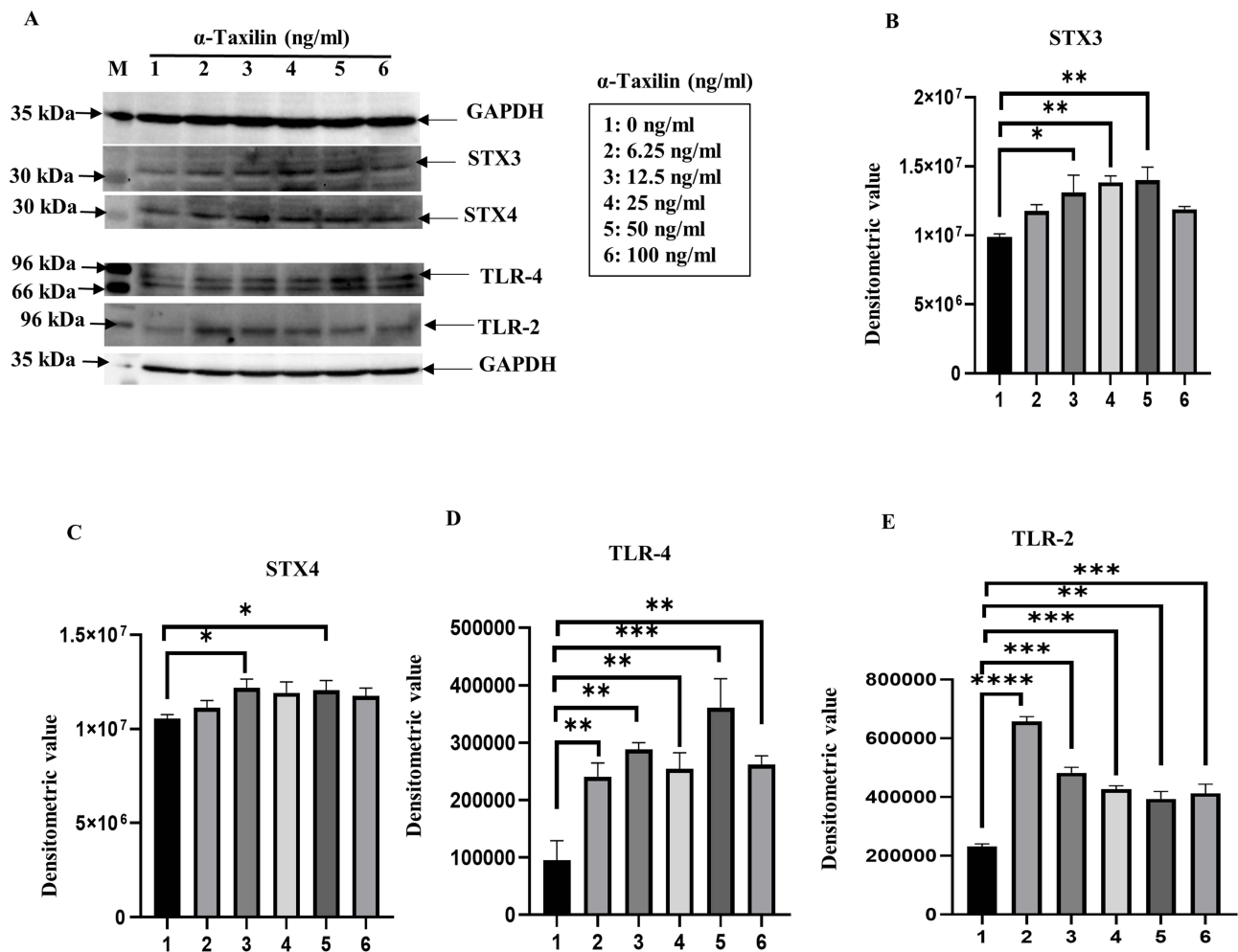


Figure 5 Effect of α -Taxilin on TLR receptor activation in RAFLS. (A) WB image showing a significant increase of STX3, STX4, TLR-2, and TLR-4 level dose-dependently upon induction with pure α -Taxilin. (B) The bar graph represents the densitometric values of WB for STX3, upregulated as we increase the dose of α -Taxilin. (C) The bar graph shows that the STX4 protein level increased as we increased the dose of α -Taxilin based on the densitometric value. (D) Increased level of TLR-4 expression in dose-dependent manner. (E) The graph represents the expression level of TLR-2 expression upon α -Taxilin induction. (* $P \leq 0.05$, ** $P \leq 0.01$, *** $P \leq 0.001$, **** $P \leq 0.0001$). **Abbreviations:** WB, Western blot; kDa, kilo Dalton; GAPDH, glyceraldehyde 3-phosphate dehydrogenase; STX3, syntaxin-3; STX4, syntaxin-4; TLR-2, toll-like receptor-2; TLR-4, toll-like receptor-4; ng, Nano gram; mL, milliliter.

panel). Paw swelling began on day 7 (Figure 7B). The paw volume was significantly increased on the 21st day in the CIA group compared to the HC group, and the group treated with siTaxilin showed a decreased paw volume compared to the CIA (Figure 7B) and NS+CIA groups. To strengthen our findings, the infiltration of immune cells into the synovium was also validated by histological analysis using H&E staining (cytosol in pink, and nucleus in blue) (Figure 7A, lower panel). Analysis of the H&E score indicated a significantly decreased number of infiltrated immune cells in siTaxilin-treated synovium compared to CIA and NS+CIA rat synovium (Figure 7C). The macroscopic arthritis score was also calculated and found to be decreased in the siTaxilin-treated group compared to that in the CIA and NS+CIA groups (Figure 7D). The inflammatory parameters were further validated by measuring pro-inflammatory cytokines by ELISA, and decreased levels of TNF- α (Figure 7E, 0.76-fold), IL-6 (Figure 7F, 0.58-fold), and IL-1 β (Figure 7G, 0.62-fold) were found in the plasma of rats in the siTaxilin group compared to those in the CIA group.

Discussion

The etiology of RA remains challenging owing to the complexity of the disease and the lack of knowledge. Exploring a less-studied biological sample or using a new technique for re-analysis can increase the possibility of finding novel biomolecules.⁴⁶ Previously we identified a novel disease-associated protein, α -Taxilin, from SF cells, which was found to

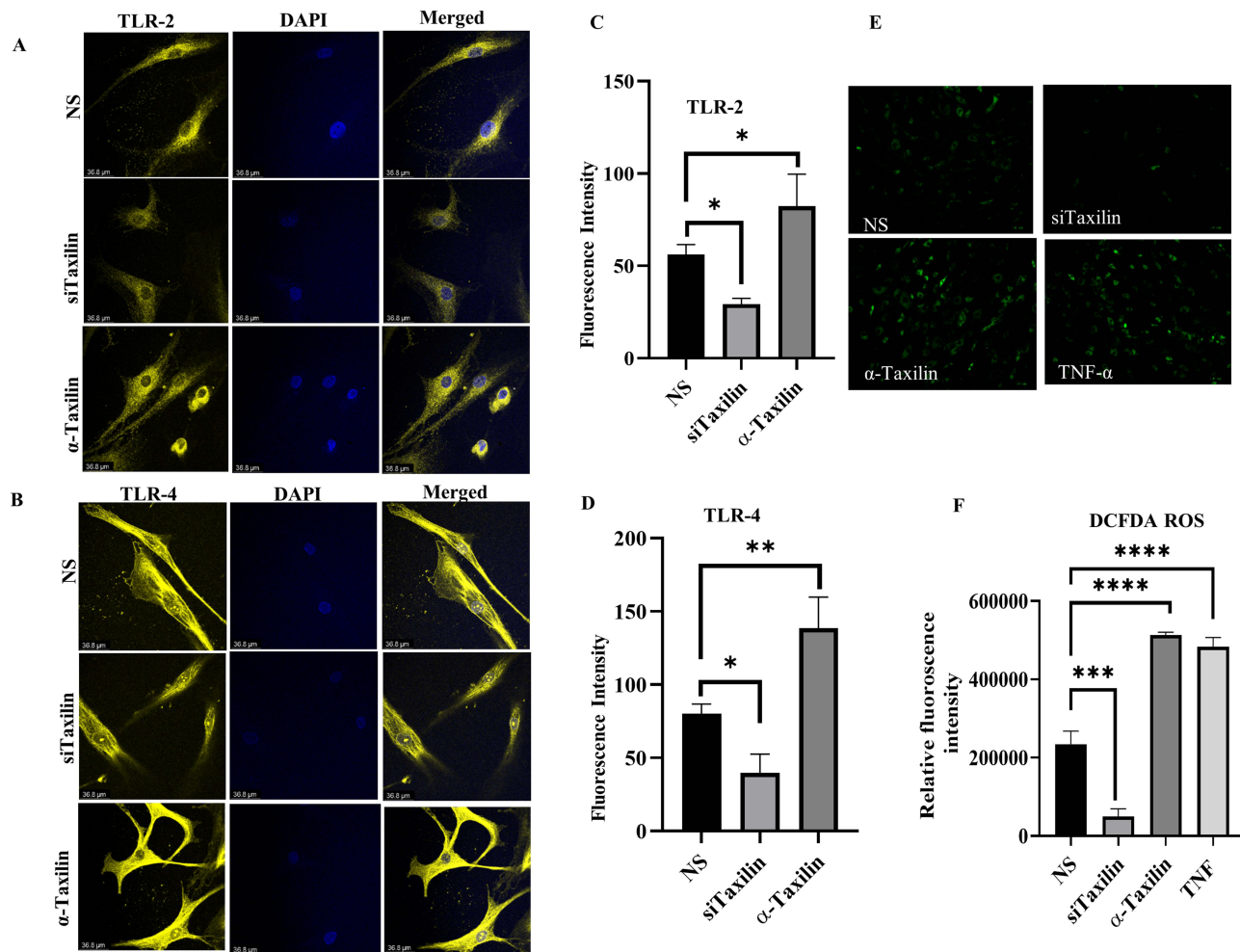


Figure 6 Effect of α -Taxilin knockdown on TLR's expression. **(A)** The confocal microscopy image shows TLR-2 expression (yellow) and nucleus (blue) in RAFLS. **(B)** The confocal microscopy image shows TLR-4 expression (yellow) and nucleus (blue) in RAFLS. **(C)** The bar graph shows the fluorescence intensity of TLR-2 expression in RAFLS after knockdown of α -Taxilin compared to the α -Taxilin and NS group. **(D)** The bar graph shows the fluorescence intensity of TLR-4 expression in RAFLS after the knockdown of α -Taxilin compared to the α -Taxilin and NS group. **(E)** The image shows fluorescence (green) of DCFDA cellular ROS production in RAFLS after knockdown of α -Taxilin, and treatment with pure recombinant α -Taxilin and the NS group. **(F)** The bar graph shows the relative fluorescence of DCFDA ROS production in the different treated groups (* $P \leq 0.05$, ** $P \leq 0.01$, *** $P \leq 0.001$, **** $P \leq 0.0001$).

Abbreviations: TLR-2, toll-like receptor-2; TLR-4, toll-like receptor-4; DCFDA, dichlorodihydrofluorescein diacetate; NS, non-specific Si-RNA; ROS, reactive oxygen species; TNF- α , Tumor Necrosis Factor- α ; DAPI, 4',6-diamidino-2-phenylindole; RAFLS, Rheumatoid arthritis fibroblast like synoviocytes.

be upregulated in RA patients, suggesting their possible involvement in disease pathology. α -Taxilin plays various roles, such as regulation of exocytosis in immune cells, regulation of the release of hepatitis virus, allograft rejection, and autoimmunity in transgenic mice.^{17,18,47} Studies have also suggested that the transcription level of α -Taxilin increases after alloantigen stimulation in organ rejection,⁴⁸ interaction with the syntaxin family, and regulation of TLRs activation, leading to the secretion of pro-inflammatory cytokines.¹⁹ To explore α -Taxilin for diagnostic purposes, we studied its concentration and found a 2-fold upregulated in RA compared to other similar inflammatory diseases (OA, and SLE) (Figure 1A) and was found to be correlated with ACPA levels, and DAS in RA patients (Figure 1C); thus, α -Taxilin was therefore explored for its role in RA pathogenesis.

The activation of the NF- κ B pathway is known to involve majorly in the manifestation of RA leading to an increase in pro-inflammatory cytokines mRNA (*IL-6*, *TNF- α* , and *IL-1 β*).⁴⁹ Cells were therefore induced with TNF- α , found up-regulation of α -Taxilin in a dose-dependent manner, and, upon siRNA treatment, a significant reduction of cytokines mRNA level compared to the TNF- α treated group in SW982 (Figure 2F–H) as well as in RAFLS (Figure 3D–F), also supported by the reduction of NF- κ B p65 level by WB (Figure 3C).

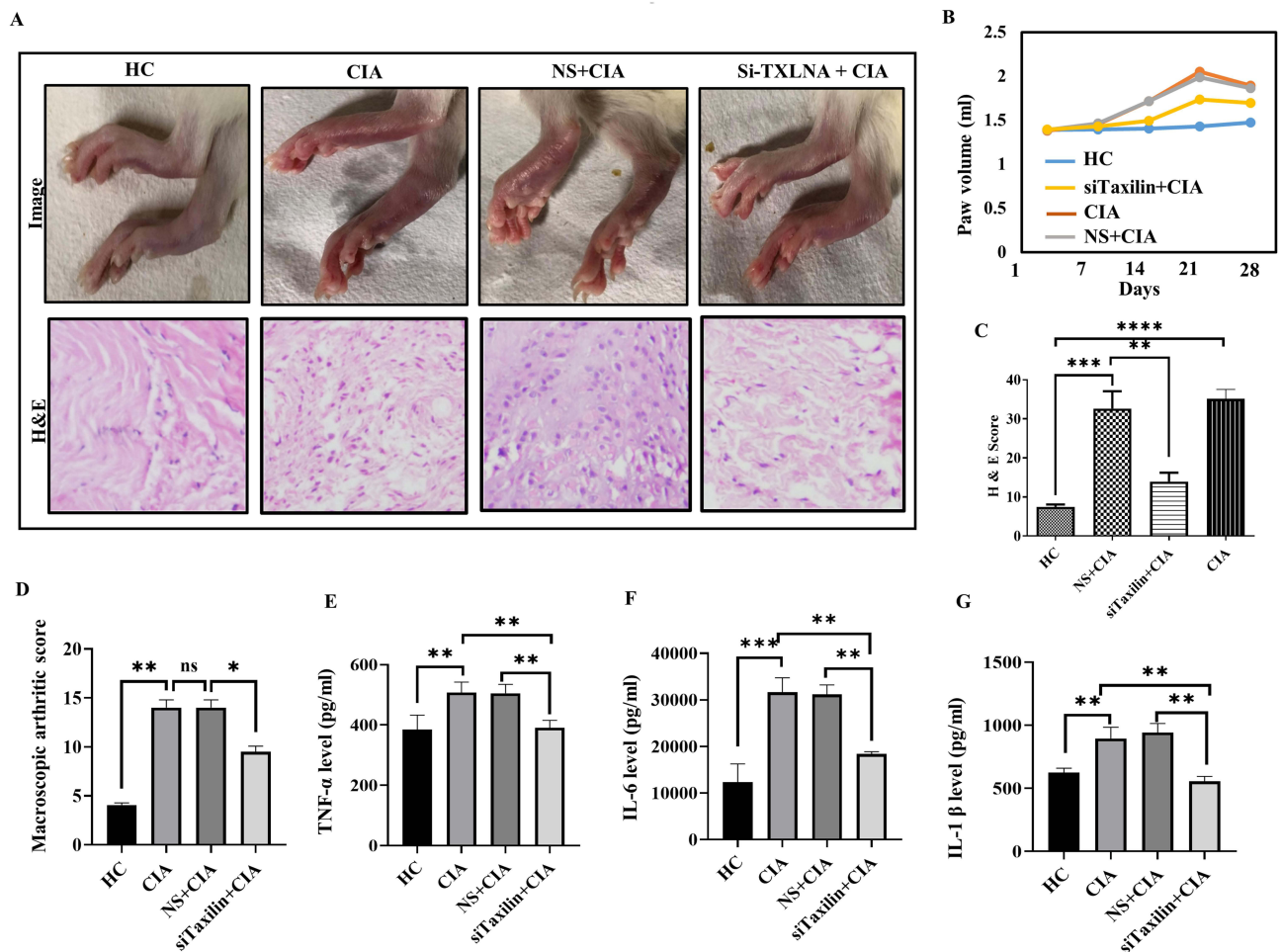


Figure 7 Alpha-Taxilin ameliorates RA-like symptom in CIA rats. **(A)** The upper panel shows a paw image taken on 28th day in HC, CIA, NS+CIA, and siTaxilin+CIA groups where the redness and swelling can be observed, whereas the lower panel shows histological evidence of cell infiltration in the synovium of respective groups. **(B)** Line graph indicating increased paw volume due to onset of inflammation and edema in CIA rats measured on day 1 to day 28 with intervals of 1 week. **(C)** The bar graph represents the infiltration of cells in the synovium of different rat groups after induction of collagen, based on calculated H&E score. **(D)** The bar graph shows macroscopic arthritis score based on macroscopic observation in rats, a decreased level of macroscopic arthritis score in the siTaxilin group compared to the CIA group was observed. **(E)** The bar graph showing TNF- α concentration in the rat's plasma sample measured by ELISA, found downregulated in the knockdown group. **(F)** The bar graph showing IL-6 concentration in rat's plasma sample measured by ELISA, found downregulated in the knockdown group. **(G)** The bar graph showing IL-1 β concentration in rat's plasma sample measured by ELISA, found downregulated in the knockdown group using siTaxilin. (* $P \leq 0.05$, ** $P \leq 0.01$, *** $P \leq 0.001$, **** $P \leq 0.0001$).

Abbreviations: HC, healthy control; NS, non-specific Si-RNA; CIA, collagen induced arthritis; H&E, Hematoxylin and Eosin; H&E, Hematoxylin and eosin staining; ns, Non-significant.

The joint inflammation of RA is closely related to the infiltration of various immune cells such as lymphocytes, mast cells, and activated macrophages in the synovium, and SF plays a central role in inflammation.⁵⁰ The increased lymphocyte infiltration in SF is correlated with increased chemokine expression.⁵¹ Natural immune cells, such as neutrophils and mast cells, contribute to the development of synovitis. Additionally, synovial tissue macrophages are involved in the immune regulation in RA, indicating possible involvement of α -Taxilin in the activation of immune cells and secretion of pro-inflammatory cytokines in RA as α -Taxilin has been found linked with activation of macrophage leads to inflammation.⁵² To find the pathways mediated by α -Taxilin in the inflammatory response, interacted proteins of α -Taxilin were co-immunoprecipitated using the Co-IP technique. The 17 proteins were identified (Table 2) by Co-IP followed by mass spectrometry. Among those many key enzymes, Fructose-bisphosphate aldolase A, ATP synthase subunit beta, L-lactate dehydrogenase A, L-lactate dehydrogenase, and Pyruvate kinase were found to be associated with glucose metabolism.⁵³ The GO and KEGG in-silico pathway enrichment was performed with identified interacted proteins. The GO enrichment indicated that cell activation, exocytosis, leukocyte-mediated immunity, and neutrophil degranulation are the molecular functions involved (Figure 4B). The GO enrichment of the biological process indicated

a major histocompatibility complex (MHC) class II protein binding complex, while cellular component enrichment indicated extracellular exosome and secretory granule by the associated proteins (Figure 4B). Further, the KEGG pathway analysis revealed “Glycolysis” and “Pyruvate metabolism”, the two major pathways (Figure 4C) associated with α -Taxilin. However, STRING analysis of the identified proteins (Supplementary data Figure S6) did not show the involvement of α -Taxilin in regulating glycolysis, indicating that α -Taxilin has not been studied in metabolic disorder-associated diseases earlier, as there is no evidence targeting the molecular mechanism of α -Taxilin related to metabolic disorders. Therefore, in order to understand its role, the mRNA expression of major glycolytic enzymes such as PKM, LDHA, and ALDOA identified by Co-IP and LC-MS/MS were validated in RAFLS. It was found that *PKM* and *LDHA* levels were upregulated in the recombinant α -Taxilin treated group (Figure 4D and E), and may be one of the factors responsible for the active metabolic shift, which is one of the crucial changes that take place in RAFLS during RA inflammation. Reports suggest that this metabolic shift onset occurs before the cell enters an inflammatory response.^{34,54} Various studies show that autoimmune Cluster of Differentiation-8 (CD8), and T-cells rely on increased LDHA activity in mediating pro-inflammatory profile in RA and aerobic glycolysis,³⁴ whereas PKM contributes TLR-mediated inflammation and autoimmunity by promoting Pyk2 activation.⁵⁴ Targeting immune metabolism for anti-inflammatory strategy, these glycolytic enzymes are gaining attention because of their involvement in autoimmune diseases.⁵⁵ The elevated activity of these enzymes leads to cellular ROS generation and TLR activation.^{56,57} The cellular ROS level was thus evaluated, and it was revealed that there is a significantly decreased level of ROS in the siTaxilin group while both α -Taxilin and TNF- α induction led to increased ROS generation in RAFLS (Figure 6F), indicating the onset of inflammation. Another report showed that α -Taxilin binds to the syntaxin family (STX3 and STX4), which may lead to TLR-2 and TLR-4, resulting in the secretion of pro-inflammatory cytokines. Therefore, we evaluated the effect of α -Taxilin on STX3 and STX4 levels and observed a significant increase in the expression of STX3 and STX4 (Figure 5B and C). Furthermore, the increased expression of TLR-2 and TLR-4 levels was also confirmed by confocal microscopy, as these are the most common receptors associated with RA-like inflammation (Figure 6A and B). These results led us to speculate that the increased levels of α -Taxilin may mediate LDHA and PKM glycolytic enzymes, leading to a metabolic shift, this may be a factor leading to the activation of TLRs (TLR-2 and TLR-4) by mediating STX3 and STX4, thus leading to the exocytosis of pro-inflammatory cytokines. Therefore, we strengthened our findings by generating CIA rat models and validating our results by the knockdown of α -Taxilin (Supplementary Figure S7). The results obtained showed a clear improvement in the macroscopic arthritis score (Figure 7D) in the siTaxilin-treated group compared to the NS+CIA group, supported by paw volume, redness measurement (Figure 7A, B, upper panel), and pro-inflammatory cytokine measurement, showing decreased levels of cytokines in the siTaxilin-treated group (Figure 7E–G). The infiltration of immune cells in the synovium is also considered a major symptom of RA,⁵⁸ similar trends were observed in our study (Figure 7C). This significant change in inflammatory markers, along with immune response-related symptoms due to α -Taxilin, indicated that α -Taxilin could be targeted for its therapeutic potential. The study also has some limitations, such as non-consideration of seronegative RA patients, non-inclusion of early RA patients, in vitro studies attempted only in fibroblast (RAFLS and SW982), and not with immune cells (Macrophages) in our study. Further study on immune cells may significantly improve the understanding of the role played by α -Taxilin in RA pathology. Further, the evaluation of α -Taxilin levels in other inflammatory diseases, such as lupus and juvenile arthritis, along with a correlation study with disease severity, may further strengthen its diagnostic potential. Although animal experiments based on the CIA model significantly mimic RA-like symptoms, however, the actual pathological symptom may significantly vary from that of human RA onset. The study can be strengthened further by doing more studies using other animal models such as proteoglycan-induced arthritis (PGIA) and collagen antibody-induced arthritis (CAIA) for further validation.⁵⁹

Conclusion

This study suggested that α -Taxilin plays a vital role in RA-like inflammation by mediating glycolytic enzymes. The decreased paw volume and macroscopic score, along with pro-inflammatory cytokines in CIA rats, indicated that α -Taxilin is one of the factors that plays a major role in mediating inflammation, which may have potential therapeutic targets to ameliorate RA-like disease progression.

Data Sharing Statement

For all original data and detailed protocols, please contact Dr Sagarika Biswas (email: sagarika.biswas@igib.res.in).

Ethical Statements Involving Human Samples

The study protocol was approved by the Medical Ethics Committee of All India Institute of Medical Sciences (AIIMS), Department of Orthopedics, New Delhi, India (AIIMS, Ref No CSIR-IGIB/IHEC2017-18 Dt.08.02.2018), and by the Council of Scientific and Industrial Research (CSIR), Institute of Genomics and Integrative Biology, Delhi, India (CSIR-IGIB/IHEC/2017-18 Dated 08.02.2018). All the study protocols complied with the Declaration of Helsinki.

Ethical Statements Involving Animals

All the animals were procured from the National Institute of Nutrition, Hyderabad, India. The experimental design was approved by the Institutional (Council of Scientific and Industrial Research - Institute of Genomics and Integrative Biology, Delhi, India) Animal Ethical Committee (Reference no: IGIB/IAEC/3/3/Mar 2023). All experiments were performed according to the IGIB-Institutional Animal Ethics Committee (IAEC) following Committee for the Purpose of Control and Supervision of Experiments on Animals (CPCSEA) guidelines and regulations.

Consent for Publication

Written signed consent was obtained from all participating patients and healthy volunteers.

Acknowledgments

We would like to thank Mr. Praveen for the mass spectrometry data acquisition. We also thank Prof. Sahil Batra (AIIMS, Delhi) for collecting the biopsy synovium and Mr. Pankaj for transporting biological samples. We acknowledge the Council of Scientific and Industrial Research (CSIR) for funding, CSIR-Institute of Genomics and Integrative Biology, and Academy of Scientific and Innovative Research (AcSIR) for providing research support.

Author Contributions

All authors made a significant contribution to the work reported, whether that is in the conception, study design, execution, acquisition of data, analysis and interpretation, or in all these areas; took part in drafting, revising or critically reviewing the article; gave final approval of the version to be published; have agreed on the journal to which the article has been submitted; and agree to be accountable for all aspects of the work.

Disclosure

The authors have no competing interests.

References

1. Weyand CM, Goronzy JJ. The immunology of rheumatoid arthritis. *Nat Immunol*. 2021;22(1). doi:10.1038/s41590-020-00816-x
2. Cross M, Smith E, Hoy D, et al. The global burden of rheumatoid arthritis: estimates from the Global Burden of Disease 2010 study. *Ann Rheum Dis*. 2014. doi:10.1136/annrheumdis-2013-204627
3. Huber LC, Distler O, Tarner I, Gay RE, Gay S, Pap T. Synovial fibroblasts: key players in rheumatoid arthritis. *Rheumatology*. 2006;45:669–675. doi:10.1093/rheumatology/kei065
4. Fang Q, Zhou C, Nandakumar KS. Review article molecular and cellular pathways contributing to joint damage in rheumatoid arthritis. *Mediators Inflamm*. 2020;2020:3830212.
5. Lin YJ, Anzaghe M, Schülke S. Update on the pathomechanism, diagnosis, and treatment options for rheumatoid arthritis. *Cells*. 2020;9(4):880. doi:10.3390/cells9040880
6. Rim YA, Ju JH. The role of fibrosis in osteoarthritis progression. *Life*. 2021;11(1):1–13. doi:10.3390/LIFE11010003
7. Köhler BM, Günther J, Kaudewitz D, Lorenz HM. Current therapeutic options in the treatment of rheumatoid arthritis. *J Clin Med*. 2019;1–15.
8. Svanström H, Lund M, Melbye M, Pasternak B. Concomitant use of low-dose methotrexate and NSAIDs and the risk of serious adverse events among patients with rheumatoid arthritis. *Pharmacoepidemiol Drug Saf*. 2018;27(8):885–893. doi:10.1002/pds.4555
9. Jin L, Wang F, Wang X, et al. Identification of plasma biomarkers from rheumatoid arthritis patients using an optimized sequential window acquisition of all theoretical mass spectra (SWATH) proteomics workflow. *Proteomes*. 2023;11(4):32. doi:10.3390/proteomes11040032
10. Biswas S, Sharma S, Saroha A, et al. Identification of novel autoantigen in the synovial fluid of rheumatoid arthritis patients using an immunoproteomics approach. *PLoS One*. 2013;8(2):e56246. doi:10.1371/journal.pone.0056246

11. Alivernini S, Bruno D, Tolusso B, et al. Differential synovial tissue biomarkers among psoriatic arthritis and rheumatoid factor/anti-citrulline antibody-negative rheumatoid arthritis. *Arthritis Res Ther.* 2019;21(1):1–11. doi:10.1186/s13075-019-1898-7
12. Hu Z, Li Y, Zhang L, et al. Metabolic changes in fibroblast-like synoviocytes in rheumatoid arthritis: state of the art review. *Front Immunol.* 2024;15. doi:10.3389/fimmu.2024.1250884
13. Fearon U, Hanlon MM, Wade SM, Fletcher JM. Altered metabolic pathways regulate synovial inflammation in rheumatoid arthritis. *Clin Exp Immunol.* 2019;197(2):170–180. doi:10.1111/cei.13228
14. de Oliveira PG, Farinon M, Sanchez-Lopez E, Miyamoto S, Guma M. Fibroblast-like synoviocytes glucose metabolism as a therapeutic target in rheumatoid arthritis. *Front Immunol.* 2019;10. doi:10.3389/fimmu.2019.01743
15. Køster D, Egedal JH, Lomholt S, et al. Phenotypic and functional characterization of synovial fluid-derived fibroblast-like synoviocytes in rheumatoid arthritis. *Sci Rep.* 2021;11(1):22168. doi:10.1038/s41598-021-01692-7
16. Sarkar A, Sharma S, Agnihotri P, et al. Synovial fluid cell proteomic analysis identifies upregulation of alpha-taxilin proteins in rheumatoid arthritis: a potential prognostic marker. *J Immunol Res.* 2020;2020:1–10. doi:10.1155/2020/4897983
17. Nogami S, Satoh S, Nakano M, et al. Taxilin; a novel syntaxin-binding protein that is involved in Ca²⁺-dependent exocytosis in neuroendocrine cells. *Genes to Cells.* 2003;8:17–28. doi:10.1046/j.1365-2443.2003.00612.x
18. Shen L, Zhang C, Wang T, et al. Development of autoimmunity in IL-14a-transgenic mice 1. *J Immunol.* 2021. doi:10.4049/jimmunol.177.8.5676
19. Nogami S, Satoh S, Tanaka-Nakadate S, et al. Identification and characterization of taxilin isoforms. *Biochem Biophys Res Commun.* 2004;319(3):936–943. doi:10.1016/j.bbrc.2004.05.073
20. Collins LE, Decourcey J, Rochfort KD, Kristek M, Loscher CE. A role for syntaxin 3 in the secretion of IL-6 from dendritic cells following activation of toll-like receptors. *Front Immunol.* 2015;5:1–9. doi:10.3389/fimmu.2014.00691
21. Raker VK, Becker C, Steinbrink K. The cAMP pathway as therapeutic target in autoimmune and inflammatory diseases. *Front Immunol.* 2016;7:1–11. doi:10.3389/fimmu.2016.00123
22. Xu C, Zhang C, Shen L, et al. Constitutive expression of interleukin 14 (IL-14) in transgenic mice leads to enhanced responses to vaccinations and autoimmunity. *J Allergy Clin Immunol.* 2005;115(2):S60. doi:10.1016/j.jaci.2004.12.252
23. Horii Y, Sakane H, Nogami S, Ohtomo N, Tomiya T, Shirataki H. Expression of α -taxilin in the murine gastrointestinal tract: potential implication in cell proliferation. *Histochemistry and Cell Biology.* 2014;141:165–180. doi:10.1007/s00418-013-1147-0
24. Fujii K, Tsuji M, Tajima M. Rheumatoid arthritis: a synovial disease? *Ann Rheum Dis.* 1999;21:727–730.
25. Kominsky DJ, Campbell EL, Colgan SP. Metabolic shifts in immunity and inflammation. *J Immunol.* 2010;184(8):4062–4068. doi:10.4049/jimmunol.0903002
26. Sarkar A, Chakraborty D, Kumar V, Malhotra R, Biswas S. Upregulation of leucine-rich alpha-2 glycoprotein: a key regulator of inflammation and joint fibrosis in patients with severe knee osteoarthritis. *Front Immunol.* 2022;13:1–13. doi:10.3389/fimmu.2022.1028994
27. Wang L, Reinach P, Lu L. TNF- α promotes cell survival through stimulation of K⁺ channel and NF κ B activity in corneal epithelial cells. *Exp Cell Res.* 2005;311(1):39–48. doi:10.1016/j.yexcr.2005.08.020
28. Sherry B, Cerami A. Cachectin/tumor necrosis factor exerts endocrine, paracrine, and autocrine control of inflammatory responses. *The Journal of Cell Biology.* 1988;107:1269–1277. doi:10.1083/jcb.107.4.1269
29. Chang J, Lee KJ, Kim SK, Yoo DH, Kang TY. Validity of SW982 synovial cell line for studying the drugs against rheumatoid arthritis in fluvastatin-induced apoptosis signaling model. *The Indian Journal of Medical Research.* 2014;139:117–124.
30. Mann S, Sharma A, Sarkar A, et al. Evaluation of anti-inflammatory effects of choerospondias axillaris fruit's methanolic extract in synoviocytes and CIA rat model. *Curr Pharm Biotechnol.* 2019;21(7):596–604. doi:10.2174/1389201021666191210114127
31. Mahmood T, Yang PC. Western blot: technique, theory, and trouble shooting. *N Am J Med Sci.* 2012;4(9):429–434. doi:10.4103/1947-2714.100998
32. Gu Z, Xia J, Xu H, Frech I, Tricot G, Zhan F. NEK2 promotes aerobic glycolysis in multiple myeloma through regulating splicing of pyruvate kinase. *J Hematol Oncol.* 2017;10:1–11. doi:10.1186/s13045-017-0392-4
33. Thompson PW, Jones DD. Serum lactic dehydrogenase as a marker of joint damage in rheumatoid arthritis. *Ann Rheumatic Dis.* 1987;46(3):263. doi:10.1136/ard.46.3.263
34. Souto-Carneiro MM, Klika KD, Abreu MT, et al. Effect of increased lactate dehydrogenase A activity and aerobic glycolysis on the proinflammatory profile of autoimmune CD8⁺ T cells in rheumatoid arthritis. *Arthritis Rheumatol.* 2020;72(12):2050–2064. doi:10.1002/art.41420
35. Singh AN, Sharma N. Quantitative SWATH-based proteomic profiling for identification of mechanism-driven diagnostic biomarkers conferring in the progression of metastatic prostate cancer. *Front Oncol.* 2020;10. doi:10.3389/fonc.2020.00493
36. Shannon P, Markiel A, Ozier O, et al. Cytoscape: a software Environment for integrated models of biomolecular interaction networks. *Genome Res.* 2003;13:2498–2504. doi:10.1101/gr.1239303
37. Agnihotri P, Saquib M, Sarkar A, Chakraborty D, Kumar U, Biswas S. Transthyretin and receptor for advanced glycation end product's differential levels associated with the pathogenesis of rheumatoid arthritis. *J Inflamm Res.* 2021. doi:10.2147/JIR.S327736
38. Amruta N, Bix G. ATN-161 ameliorates ischemia/reperfusion-induced oxidative stress, fibro-inflammation, mitochondrial damage, and apoptosis-mediated tight junction disruption in bend. 3 Cells. *Inflammation.* 2021;44(6):2377–2394. doi:10.1007/s10753-021-01509-9
39. Xie FY, Woodle MC, Lu PY. Harnessing in vivo siRNA delivery for drug discovery and therapeutic development. *Drug Discovery Today.* 2006;11(1):67–73. doi:10.1016/S1359-6446(05)03668-8
40. Singh K, Gupta A, Sarkar A, et al. Arginyltransferase knockdown attenuates cardiac hypertrophy and fibrosis through TAK1-JNK1/2 pathway. *Sci Rep.* 2020;10(1):1–11. doi:10.1038/s41598-019-57379-7
41. Hu Y, Yang YI, Luo BIN. Evaluation of destruction in a collagen - induced arthritis rat model: bony spur formation. *Exp Ther Med.* 2017;2563–2567. doi:10.3892/etm.2017.4817
42. Feldman AT, Wolfe D. Chapter 3 tissue processing and hematoxylin and eosin staining. In: Feldman AT, Wolfe D, editors. *Tissue Processing and Staining.* vol. 1180. 2014:31–43. doi:10.1007/978-1-4939-1050-2
43. Sarkar A, Kumar V, Malhotra R, et al. Poor clearance of free hemoglobin due to lower active haptoglobin availability is associated with osteoarthritis inflammation. *J Inflamm Res.* 2021;14:949–964. doi:10.2147/JIR.S300801
44. Beyleveld G, White KM, Aylton J, Shaw ML. New-generation screening assays for the detection of anti-influenza compounds targeting viral and host functions. *Antiviral Res.* 2013;100(1):120–132. doi:10.1016/j.antiviral.2013.07.018
45. Yang S, Lian G. ROS and diseases: role in metabolism and energy supply. *Mol Cell Biochem.* 2020;467(1–2):1–12. doi:10.1007/s11010-019-03667-9

46. Baird AL, Westwood S, Lovestone S. Blood-based proteomic biomarkers of Alzheimer's disease pathology. *Front Neurol*. 2015;6. doi:10.3389/fneur.2015.00236
47. Hoffmann J, Boehm C, Himmelsbach K, et al. Identification of a -taxilin as an essential factor for the life cycle of hepatitis B virus. *J Hepatol*. 2013;59(5):934–941. doi:10.1016/j.jhep.2013.06.020
48. Leca N, Laftavi M, Shen L, Matteson K, Ambrus J, Pankewycz O. Regulation of human interleukin 14 transcription in vitro and in vivo after renal transplantation. *Transplantation*. 2008;86(2):336–341. doi:10.1097/TP.0b013e31817c6380
49. Makarov SS. NF- κ B in rheumatoid arthritis: a pivotal regulator of inflammation, hyperplasia, and tissue destruction. *Arthritis Res*. 2001;3(4):200–206. doi:10.1186/ar300
50. Tu J, Huang W, Zhang W, Mei J, Zhu C. A tale of two immune cells in rheumatoid arthritis: the crosstalk between macrophages and T cells in the synovium. *Front Immunol*. 2021;12:1–8. doi:10.3389/fimmu.2021.655477
51. Koo J, Kim S, Jung WJ, et al. Increased lymphocyte infiltration in rheumatoid arthritis is correlated with an increase in LTi-like cells in synovial fluid. *Immune Netw*. 2013;13(6):240–248. doi:10.4110/in.2013.13.6.240
52. Luo P, Wang P, Xu J, et al. Immunomodulatory role of T helper cells in rheumatoid arthritis. *Bone Joint Res*. 2022;11(7):426–438. doi:10.1302/2046-3758.117.BJR-2021-0594.R1
53. Beylerli O, Sufianova G, Shumadalova A, Zhang D, Gareev I. MicroRNAs-mediated regulation of glucose transporter (GLUT) expression in glioblastoma. *Non-Coding RNA Res*. 2022;7(4):205–211. doi:10.1016/j.ncrna.2022.09.001
54. Alves-filho JC, Pålsson-mcdermott EM, Alves-filho JC, Pålsson-mcdermott EM. Pyruvate kinase M2: a potential target for regulating inflammation. *Front Immunol*. 2016;7:1–7. doi:10.3389/fimmu.2016.00145
55. Pålsson-mcdermott EM, Neill LAJO. Targeting immunometabolism as an anti-inflammatory strategy. *Cell Res*. 2020;30:300–314. doi:10.1038/s41422-020-0291-z
56. Chen Z, Zhong H, Wei J, et al. Inhibition of Nrf2/HO-1 signaling leads to increased activation of the NLRP3 inflammasome in osteoarthritis. *Arthritis Res Ther*. 2019;21(1):1–13. doi:10.1186/s13075-019-2085-6
57. Krawczyk CM, Holowka T, Sun J, et al. Toll-like receptor-induced changes in glycolytic metabolism regulate dendritic cell activation. *Blood*. 2010;115(23):4742–4749. doi:10.1182/blood-2009-10-249540
58. Zhou S, Lu H, Xiong M. Identifying immune cell infiltration and effective diagnostic biomarkers in rheumatoid arthritis by bioinformatics analysis. *Front Immunol*. 2021;12:1–13. doi:10.3389/fimmu.2021.726747
59. Pandey S. Various techniques for the evaluation of anti arthritic activity in animal models. *J Adv Pharm Technol Res*. 2010;1(2):164–171. doi:10.4103/2231-4040.72254

Publish your work in this journal

The Journal of Inflammation Research is an international, peer-reviewed open-access journal that welcomes laboratory and clinical findings on the molecular basis, cell biology and pharmacology of inflammation including original research, reviews, symposium reports, hypothesis formation and commentaries on: acute/chronic inflammation; mediators of inflammation; cellular processes; molecular mechanisms; pharmacology and novel anti-inflammatory drugs; clinical conditions involving inflammation. The manuscript management system is completely online and includes a very quick and fair peer-review system. Visit <http://www.dovepress.com/testimonials.php> to read real quotes from published authors.

Submit your manuscript here: <https://www.dovepress.com/journal-of-inflammation-research-journal>